Journal of Colloid and Interface Science 331 (2009) 555–559

Contents lists available at ScienceDirect

Journal of Colloid and Interface Science

www.elsevier.com/locate/jcis

Short Communication

Crown-forming instability phenomena in the drop splash problem

Rouslan Krechetnikov [a,1], George M. Homsy [b,*]

[a] Department of Mathematics, University of Alberta, Edmonton, Canada
[b] Department of Mechanical Engineering, University of California, Santa Barbara, USA

ARTICLE INFO

Article history:
Received 7 August 2008
Accepted 14 November 2008
Available online 16 December 2008

Keywords:
Drop splash
Crown formation
Rim instability
Frustration phenomena

ABSTRACT

The objective of this work is to study the fundamental instability behind the crown formation in the problem of drop splashing on a pre-existing liquid film. Based on experimental and theoretical insights, we demonstrate that the most plausible instability mechanism is of the Richtmyer–Meshkov type associated with a nearly impulsive acceleration of the interface. We also discover frustration phenomena in the wave number selection of the crown spike structure and study the corresponding bifurcation picture.

1. Introduction

The drop splash problem has always fascinated scientists, as evidenced by the ongoing interest in it by the scientific community. The original motivation for our work comes from the question of Betyaev [1] as to why there are exactly 24 spikes in the famous photo of the milk crown by Edgerton and Killian [2]. As our experiments demonstrate, this question can be generalized as follows: why for some physical parameters is the crown regular with its spikes uniformly redistributed along the rim, and their number constant, while for other values of the physical parameters the crown appears disordered? The answer to this question naturally relies on a second even more fundamental question: what is the instability mechanism underlying the crown formation? While the first question has never been tackled either theoretically or experimentally, the second question, i.e. the nature of instability, has been much discussed in the literature, in particular in the context of a drop splashing on wet surfaces as studied here.

As Fullana and Zaleski [3] commented, the instability mechanism remains undetermined. In the review paper by Yarin [4], only two competing theories are mentioned: (a) the capillary instability of the rim, considered as a toroidal thread, and (b) the bending instability of the toroidal rim. Fullana and Zaleski [3] put forward the idea that the crown formation in problems like drop splashing on thin films is due to the Plateau–Rayleigh (RP) capillary instability of the cylindrical rim that develops at the end of the planar sheet. Their analytical study, based on one-dimensional macroscopic balance, showed that "the growing cylindrical end rim does not typically break into droplets for moderate wavelength," i.e. the authors could not detect an instability with their model. Gueyffier and Zaleski [5] speculated that a possible instability mechanism in a drop splashing on thin liquid films might be of the Richtmyer–Meshkov (RM) type as opposed to the Rayleigh–Taylor (RT) instability[2] deemed present in the drop splashing on dry surfaces [6], but did not provide any evidence to support or refute the conjecture.

To date the drop splash problem has been studied most extensively by experimental means, e.g. [7–10]. Despite these and many other experimental studies, the instability mechanism responsible for the crown formation and the details of the crown spike dynamics remain open questions.

2. Experimental set-up

In this work we focus on a drop splash on a film of the same liquid; as a result, the experimental set-up is very simple, as can be seen from the sketch in Fig. 1. A high-speed camera (HSC) Phantom V 5.1 with adjustable angle and distance of view provides a record of the phenomena. The drop splash takes place on a film of liquid in a Petri dish, which is placed on a high-precision digital balance Ohaus Explorer Pro EP612C, which allows one to measure the film thickness gravimetrically. The drop is released from a known height from a syringe of the diameter 2 mm attached to a pump (MasterFlex) and mounted over the dish. The use of the

* Corresponding author. Fax: +1 (805) 893 8651.
E-mail address: bud@engineering.ucsb.edu (G.M. Homsy).
[1] Current address: Department of Mechanical Engineering, University of California, Santa Barbara, USA.

[2] We recall that the basic difference between the RM and the RT instabilities is the sudden acceleration of the interface in RM as opposed to a constant acceleration in RT. The former allows for the development of interfacial instability regardless of the direction of acceleration.

0021-9797/$ – see front matter
doi:10.1016/j.jcis.2008.11.079

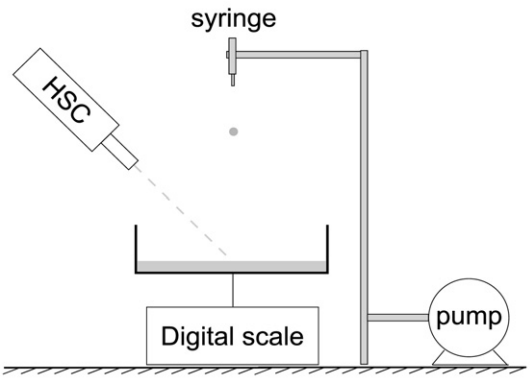

Fig. 1. Experimental set-up. A drop of size d is released from a height H onto a layer of thickness h of the same liquid.

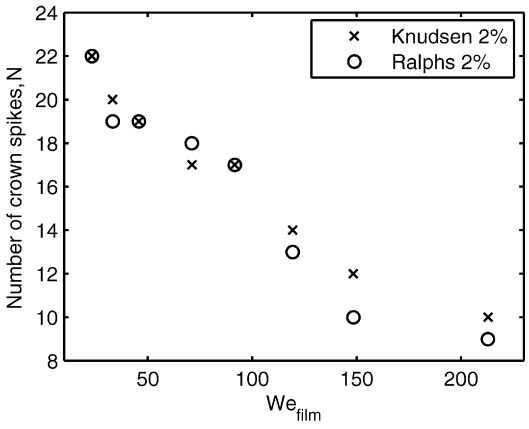

Fig. 2. Comparison of two different milks; release height is 16.5 cm; drop diameter is 4.8 mm.

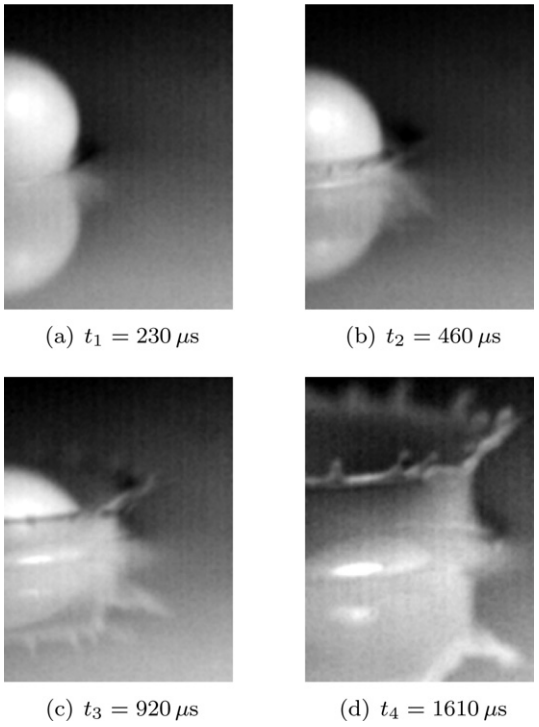

Fig. 3. Crown formation: from ejecta to crown; t_{1-4} are the times elapsed from the moment of drop impact.

pump allows one to produce a sequence of drops of a uniform size and thus to get statistics by performing several splashes under the same physical conditions. The drops were released at very slow rate, so that the drops are of uniform size[3] and the film fully relaxes between impacts. The drop diameter d, which is very nearly constant, is 4.4 mm in the case of water, while in the case of milk it is 4.8 mm.[4]

It should be noted that the HSC Phantom V 5.1 has the capability of capturing up to 96,000 frames per second (fps), which makes it possible to measure accurately the kinematics of the early stages of a drop impact; the pixel resolution at this fastest speed is however only 64×32. In reality, the inevitable compromise between spatial resolution and speed limits us to time scales on the order of 50 μs.

If one neglects the influence of surrounding air, the governing physical variables are the fluid properties ρ, μ, and σ (density, dynamic viscosity, and surface tension, respectively), the physical lengths d, h, and H (drop size, layer thickness, and height of the drop release measured from the tip of the nozzle), and the acceleration of gravity g. Since we work with fluids with comparable viscosities, the Ohnesorge number $Oh = \mu/\sqrt{\sigma\rho d} \simeq (0.15\text{–}0.41) \times 10^{-2}$, which measures the ratio of viscous and capillary forces, does not vary significantly. Thus we have a two parameter problem, controlled by the Weber number $We_{\text{drop}} = \rho v^{*2} d/\sigma \simeq (0.6\text{–}14) \times 10^2$, which relates inertial to capillary forces, and the inertia ratio $\alpha = d/h \simeq 0.1\text{–}10.0$ (or $We_{\text{film}} = \alpha^{-1} We_{\text{drop}}$), where $v^* = \sqrt{2gH} \simeq 1.0\text{–}3.6$ m/s is the impact velocity.

Since this work was motivated by the questions regarding the milk crown produced by Edgerton and Killian [2], it is natural to perform experiments with milk as well as water. While milk is probably not the best choice for quantitative experiments, since it is not a chemically well-defined liquid, our studies showed (i) the repeatability and independence of the results on a particular commercial source and (ii) that the generic bifurcation behavior is qualitatively the same as for water. The former can be seen in Fig. 2, where we show the number of spikes in the crown as a function of We_{film} for two different sources of milk, and the latter will be discussed later in the context of Fig. 6. The viscosity of the milk used in our experiments is 1.84 times higher than the viscosity of water at temperature of 25°, as measured using a Cannon–Fenske viscometer. Finally, the surface tension σ of a milk at the air interface was determined by the pendant drop method [12] and was found to be 39.9 mN/m, which is considerably lower than that of water, $\sigma_{\text{water}} = 72.0$ mN/m, which is the major (∼90%) constituent of milk. These values naturally suggest that milk contains surface active substances.

3. Results

Our experimental studies focused on the generic case of the crown formation, which is shown in Fig. 3 as a time sequence. Very shortly after initial impact, an ejecta, i.e. a thin sheet of liquid, is thrown out radially and vertically outward, as can be seen in Figs. 3(a) and 3(b). The crown is then formed from the subsequent evolution of the ejecta, as illustrated in Figs. 3(c) and 3(d). Similar to other authors [7], we refer to both physically observable cases with and without spikes as *crowns* (with and without break-up in the terminology of Rioboo et al. [7]). We now discuss the bifurcation phenomena and the nature of the instability responsible for the formation of a crown.

[3] It is known from the classical work of Shaw [11] that at higher flow rates the drops may be of different size.

[4] While it is intuitive that higher surface tension of water should be able to hold a larger drop, the milk (with lower surface tension than that of water) has different wettability properties, which result in different boundary conditions at the interface with the syringe, leading to slightly larger drops.

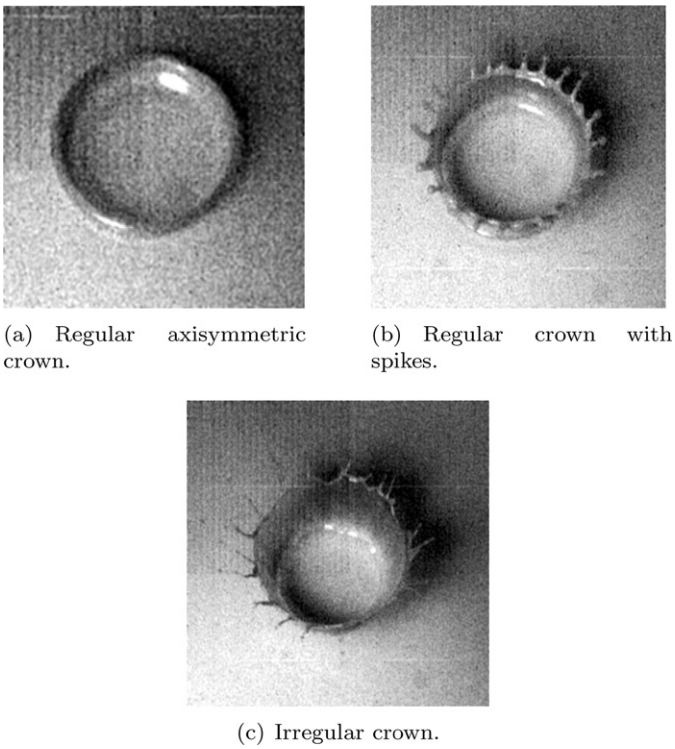

(a) Regular axisymmetric crown.

(b) Regular crown with spikes.

(c) Irregular crown.

Fig. 4. Three modes of a crown formation: late stages.

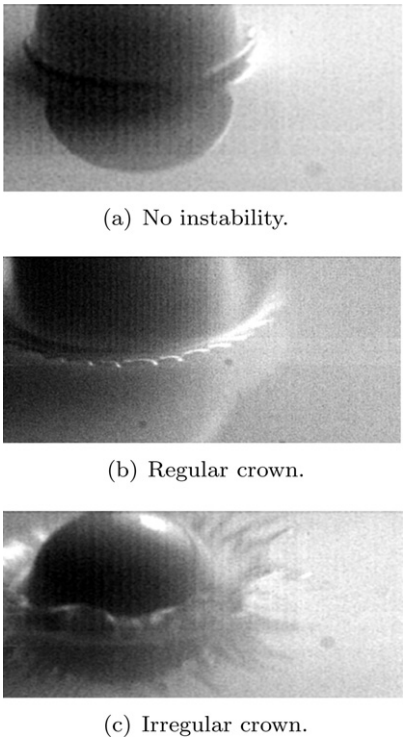

(a) No instability.

(b) Regular crown.

(c) Irregular crown.

Fig. 5. Three modes of a crown formation: early stages. The images are taken within a few hundred microseconds after impact.

3.1. Bifurcation phenomena

A large number of experiments were conducted with both water and milk over a range of *We* and α. Depending upon these parameters, there are three broad classes of behavior illustrated in Figs. 4–5 showing late and early stages of crown development: (1) no instability (the rim remains axisymmetric) as in Figs. 4(a) and 5(a); (2) regular spike formation with a well-defined wavelength as in Figs. 4(b) and 5(b); and (3) irregular spike formation such as in Figs. 4(c) and 5(c). Fig. 4 shows these at later times when the crowns are well developed. In support of this visual perception, the notions of *regular* and *irregular* will be made precise below. An important discovery is that the type of crown formation (i.e. regular or irregular) is generally dictated at the *very early stages* of the ejecta formation. By comparing the late and early stages of the crown evolution in Figs. 4 and 5, respectively, we find that if the ejecta is regular without, cf. Fig. 5(a), or with, cf. Fig. 5(b), spikes in the first moments of its appearance, it evolves into regular axisymmetric, cf. Fig. 4(a), or spiked, cf. Fig. 4(b), crowns, respectively. The same applies to the irregular ejecta regime. This behavior is *generic* and occurs over a wide range of parameters.

The above observations suggest that the ejecta exhibits some distinct properties at the early stages which in turn dictate the dynamics of the later ejecta evolution. As one can guess, the early kinematic properties of the ejecta — its velocity and acceleration — are the most prominent compared to the ones in the late stages, as will be discussed in Section 3.2.

The corresponding bifurcation picture of the crown formation is far from being trivial, as can be seen through a study of the number of spikes, N, in the crown as a function of We_{drop}, cf. Fig. 6. However, the value of N alone masks other important features such as whether the crown is regular or irregular and whether the wavelength of the distribution of spikes along the crown rim is unique. Fig. 6 shows such bifurcation picture for the milk crown; qualitatively the same picture takes place for the water crown, but with different transition values of the *We* numbers. By definition, N is zero for axisymmetric crowns. Above a certain critical

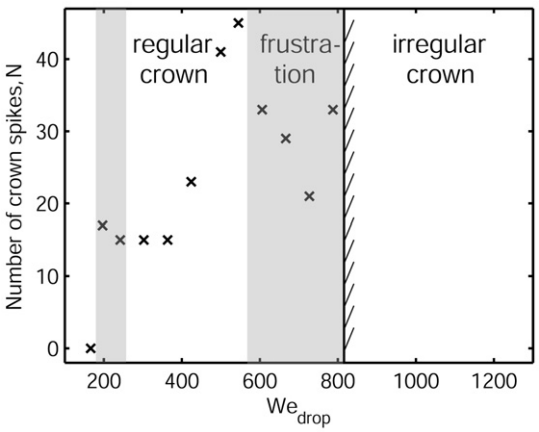

Fig. 6. Intermittency of frustration and regular regimes (shaded regions correspond to the frustration regimes) in the milk crown; film thickness 0.89 mm; drop diameter is 4.8 mm; $We_{\text{film}} = 30.9$–224.6.

value We_{drop}, dependent on α, the number of spikes generally increases. With further increase in We_{drop}, the distribution of the spikes along the rim changes from *regular*, when there is one distinct wavelength, to *irregular*, where it is difficult to discern well-defined wavelengths. This transition has intermittent states of *frustration* [13], i.e. when two or three wavelengths compete with each other, as shown in Fig. 7. When there are more than three wavelengths, it becomes difficult to distinguish the wavelength structure, which suggests that the transition to the irregular spatial structure regime might be sharp.

The frustration and regular regimes can also alternate as can be seen from Fig. 6. The system shows sensitivity to initial conditions, although in the "regular" regime the number of spikes is insensitive to the details of the initial conditions but rather is determined by the physical parameters discussed in Section 2. In this respect, the splash in the famous photo of the milk crown by Edgerton and

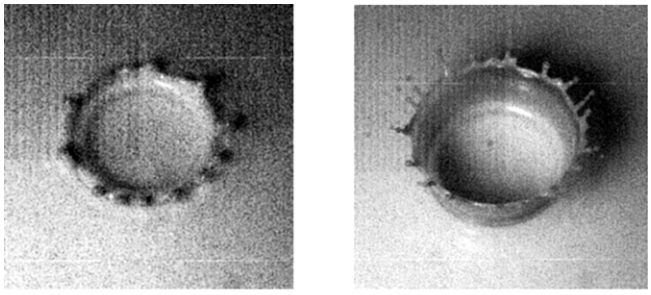

(a) Release height 12.7 cm; $We_{\mathrm{drop}} = 302.5$.

(b) Release height 37 cm; $We_{\mathrm{drop}} = 877$.

Fig. 7. Frustration phenomena: frustration patterns are characterized by (a) two or (b) three competing wavelengths of the spikes distribution along the crown rim.

Killian [2] occurs in the parameter range corresponding to the regular crown regime, and the occurrence of exactly 24 spikes is explained by a particular choice of We_{drop} and α. However, it should be stressed that there is no theory currently available which would predict the number of spikes at this moment since neither the RT nor RM instability is understood for highly curved interfaces.

3.2. Instability mechanism

Fig. 8(a) shows the position of the tip of the interface, measured along its trajectory, as a function of time, while Fig. 8(b) gives the velocity versus time. In both cases, the first non-zero data point is at approximately 100 μs. These data were generated by image analysis of the crown rim trajectory in movies produced at 13,029 fps and are similar to those obtained for drop impact on dry solid surfaces [14,15].

In view of the fact that the ejecta is a material object possessing mass, it cannot be accelerated instantaneously to reach non-zero velocity at $t = 0$, since this would contradict the fundamental physical law of energy conservation. On the other hand, obviously, the ejecta was not existing as an entity before the impact, i.e. a mass moving with finite non-zero velocity. In fact, experiments show that the ejecta originates from the film fluid [8], which is at rest for $t \leqslant 0$; thus forces must be involved to bring it to the moving state, i.e. acceleration but not deceleration should take place for $t \to 0^+$, and the initial ejecta velocity at $t = 0$ is zero. As one can clearly see from Fig. 8(b), the time period over which the acceleration happens is very short, certainly less than 100 μs. Below we first discuss some of the essential physics of this process relevant to the subsequent analysis of the instability mechanisms.

First of all, the ejecta experiences a very large acceleration in an approximately impulsive manner, as can be seen from Fig. 8. Fig. 8(b) indicates that the maximum ejecta velocity can be several times higher in magnitude than the impact velocity, in agreement with the early observations of Thoroddsen [8]. The peak values of acceleration are at least on the order of 10^5 m/s^2, as estimated from Fig. 8. Such a large acceleration is possible due to the small mass of the ejecta which is formed in the early stage of an impact. The above value of acceleration is in fact an underestimate; the key point is that there is a nearly impulsive acceleration.

In order to appreciate the importance of the early stages of ejecta evolution in the crown formation, let us consider the general picture of the collision of a drop with a liquid surface leading to a splash, i.e. so-called splashing mode (as opposed to drop spreading and bouncing regimes), depicted in Fig. 9, which is consistent with that of others, e.g. the theoretical considerations of Rein [16] and the axisymmetric numerical simulations of Josserand and Zaleski [17]. Three key elements occur with a time scale smaller than milliseconds. First, cf. Fig. 9(a), the drop must coalesce with the liquid film in an inertia-dominated manner, since $We_{\mathrm{drop}} \gg 1$

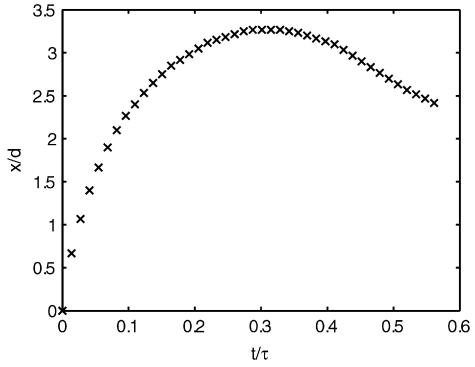

(a) Displacement.

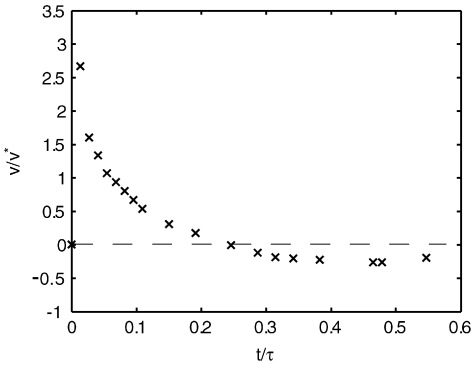

(b) Velocity.

Fig. 8. Crown rim kinematics: impact velocity is 1.8 m/s; drop size is 4.8 mm; film thickness is 0.9 mm; the characteristic time $\tau = \sqrt{d^3\rho/\sigma} \simeq 10^{-2}$ s.

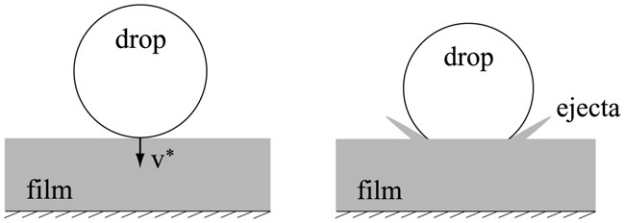

(a) Inertia-dominated impact.

(b) Formation of ejecta.

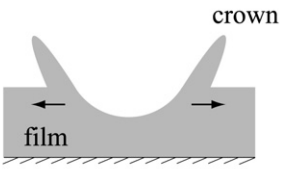

(c) Crown evolution.

Fig. 9. Schematics of three key elements of the drop splash.

in our case (cf. Section 2). Second, cf. Fig. 9(b), the vertically-downward directed momentum of the drop must be conserved and, in our problem, may be redistributed between two components, downward and upward ones. The downward component is carried by the obstruction, i.e. the liquid and the support (dish, scale, etc.). The upward component is carried by the vertically directed ejected liquid. The latter has the following origin: once the drop impacts the surface, a layer of displaced liquid beneath it moves radially and since it fails to accelerate the bulk of surround-

ing liquid, this layer is deflected upwards and forms an ejecta, also known as jetting. It is at this stage that the interface of the ejecta is accelerated nearly impulsively, i.e. the aforementioned radial movement of the fluid in the bulk is not itself responsible for the instability. Thus, shortly after the impact a thin film of targeted liquid is ejected upward at the periphery of the drop. Third, cf. Fig. 9(c), due to the intrusion of the drop, the film liquid is displaced radially. Thus, a cavity is formed in the target liquid which then expands to form a crater of a hemispherical shape at the periphery of which a sheet of liquid, originating from the ejecta as illustrated in Fig. 3, is raised above the film surface and forms the crown.

With the above understanding of the role of ejecta in the crown formation, we recall our observations in Fig. 5 that the instability occurs, if at all, during the time interval between impact and the first frame thereafter, typically within the first 100 μs or so. We further recall that the number of spikes in the crown is clearly visible at this time, and the crown generally evolves thereafter with the same number of spikes in the regular crown regime. Thus, the instability mechanism is operative in the first fractions of a millisecond. Since at the early stage of an impact the heavier fluid (water) is accelerated into the lighter one (air), naturally followed by deceleration with respect to the air phase, one can conclude that the Rayleigh–Taylor instability, if operative, should be preceded by the Richtmyer–Meshkov instability. Moreover, based on the growth rates analysis one can show from purely kinematic considerations that the RT instability is dominated by the RM instability over the time period during which the wavenumber selection is done, i.e. the time over which the spike structure is set. Concluding, the rim instability develops as follows:

- first, the liquid is nearly impulsively accelerated into the air and thus is RM unstable, which leads to a selection of a wavenumber;
- second, when the interface is decelerating, the RT instability amplifies the interface corrugations thanks to the curvature effect (see also the discussion on the first page of Sharp [18]), but does not lead to a change of the number of spikes.

In view of the above observations, the process envisioned in [3,19] and other works does not take place over the range of parameters studied here. These authors hypothesized that *first* there is a flat edge, *then* the interface retracts and a blob forms and breaks up via Rayleigh–Plateau mechanism. In reality, the well-developed instability is visible as close to the very beginning as we are able to measure and based on the general theory of the RM instability should take place immediately following the moment of impact. Given the fact that the ejecta experiences a nearly impulsive acceleration and that there is no critical physical parameter at which instability occurs, i.e. the RM instability always takes place as long as there is an impulse, the ejecta is undoubtedly subject to a RM instability. As argued above, at later times when the ejecta is decelerated, the RT mechanism amplifies the interfacial corrugations produced by the RM instability but generally does not change the wavenumber structure. The picture we see at the time, $t \simeq 100$ μs, say in Fig. 5(b), is the result of this process.

4. Conclusions

With the help of a set of experiments and new theoretical understanding we were able to gain new insights into the nature of the instability responsible for the crown spike formation, as well as into the peculiarities of the crown evolution. In particular, we discovered that there are three major types of crowns — axisymmetric, regular, and irregular — and their selection is done at the very early stages of ejecta formation. Through estimates of growth rates and our kinematic measurements, the Richtmyer–Meshkov instability mechanism is found to play a dominant role at short times. The crown dynamics also exhibits a nontrivial bifurcation behavior, which includes frustration and irregular crown phenomena.

The above observations require new theoretical advances both at the linear and nonlinear levels of description in order to achieve a complete fundamental understanding of the crown formation and a quantitative comparison with experiments.

Acknowledgments

This work was supported by a grant from the National Science Foundation, NSF/CTS 0245396, and NSERC Discovery Grant 341849. We also thank the IMMS, funded by Los Alamos National Laboratory, for use of the high speed camera. The authors appreciate the comments from Martin Rein. R.K. is also grateful to Edgar Knobloch for the discussion on the frustration phenomena.

References

[1] S.K. Betyaev, Phys. Uspekhi 38 (1995) 287–316.
[2] H.E. Edgerton, J.R. Killian, Flash! Seeing the Unseen by Ultra High-Speed Photography, Charles T Branford Co., Boston, 1954.
[3] J.M. Fullana, S. Zaleski, Phys. Fluids 11 (1999) 952–954.
[4] A.L. Yarin, Annu. Rev. Fluid Mech. 38 (2006) 159–192.
[5] D. Gueyffier, S. Zaleski, C. R. Acad. Sci. Paris Ser. II 326 (1998) 839–844.
[6] R.F. Allen, J. Colloid Interface Sci. 51 (1975) 350–351.
[7] R. Rioboo, C. Bauthier, J. Conti, M. Voué, J.D. Coninck, Exp. Fluids 35 (2003) 648–652.
[8] S.T. Thoroddsen, J. Fluid Mech. 451 (2002) 373–381.
[9] G.E. Cossali, M. Marengo, A. Coghe, S. Zhdanov, Exp. Fluids 36 (2004) 888–900.
[10] A.-B. Wang, C.-C. Chen, Phys. Fluids 12 (2000) 2155–2158.
[11] R.S. Shaw, The Dripping Faucet as a Model Chaotic System, Arial, Santa Cruz, 1984.
[12] A.W. Adamson, Physical Chemistry of Surfaces, Wiley, New York, 1990.
[13] S. Residori, N. Olivi-Tran, E. Pampaloni, Eur. Phys. J. D 12 (2000) 15–20.
[14] O.G. Engel, J. Appl. Phys. 44 (1972) 692–704.
[15] C.D. Stow, M.G. Hadfield, Proc. R. Soc. London A 373 (1981) 419–441.
[16] M. Rein, Fluid Dyn. Res. 12 (1993) 61–93.
[17] C. Josserand, S. Zaleski, Phys. Fluids 15 (2003) 1650–1657.
[18] D.H. Sharp, Physica D 12 (1984) 3–18.
[19] I.V. Roisman, K. Horvat, C. Tropea, Phys. Fluids 18 (2006) 102104.